Journal of Nuclear Materials 155-157 (1988) 715-721
North-Holland, Amsterdam

COMPATIBILITY OF FERRITIC STEELS IN FORCED CIRCULATION LITHIUM AND Pb-17Li SYSTEMS *

O.K. CHOPRA [1] and D.L. SMITH [2]

[1] *Materials and Components Technology Division,* [2] *Fusion Power Program, Argonne National Laboratory, Argonne, IL 60439, USA*

Corrosion data are presented for various ferritic steels in flowing lithium and Pb-17Li environments at temperatures between 371 and 538 °C. The corrosion behavior is evaluated by measuring weight loss as a function of time and temperature. The influence of chemical interactions between nitrogen and alloy elements on the corrosion behavior in lithium is discussed.

1. Introduction

Liquid lithium and the eutectic Pb-17 at% Li alloy have been proposed as the tritium breeder as well as the coolant for fusion reactors that operate on the D-T fuel cycle. Lithium is attractive because of its acceptable tritium-breeding and efficient heat transfer characteristics. The Pb-17Li alloy is of interest because of neutron multiplication in lead, which enhances tritium-breeding performance, and the low reactivity of the alloy with air and water relative to that of liquid lithium. Two major concerns arising from the use of lithium or Pb-17Li for tritium breeding and heat transfer are corrosion/mass transfer and the effects these substances have on the mechanical properties of the containment material. The corrosion behavior of several ferritic and austenitic steels has been investigated in liquid lithium and Pb-17Li loops; and the influence of various material and system parameters has been identified [1-16]. The results indicate that corrosion product mass transfer and deposition may determine the maximum operating temperature in some liquid-metal blanket systems.

The ferritic HT-9 alloy and Fe-9Cr-1Mo steels exhibit better resistance to corrosion than the austenitic steels such as Type 316 stainless steel. In flowing lithium systems, the dissolution rates of ferritic steels reach a constant value after an initial transient period of ~ 500 h that is characterized by rapid dissolution [1,2]. The dissolution rates increase with an increase in temperature. An Arrhenius plot of the dissolution rates for HT-9 and modified Fe-9Cr-1Mo steel yields an activation energy of 68.2 kJ/mol (16.3 kcal/mol) [2]. During the initial transient period, the alloy surfaces develop a dimpled appearance that is associated with depletion of chromium from the steel. The corrosion data also indicate that dissolution of major alloy elements as well as chemical reactions, e.g., between nitrogen and chromium or iron, influence the dissolution behavior of ferrous alloys in lithium.

The weight loss and dissolution rates of ferritic steels in flowing Pb-17Li are an order of magnitude greater than in lithium [3,4]. The large weight loss during the initial transient period is significant only at temperatures > 450 °C. The steady-state dissolution rate data for ferritic steels exposed to Pb-17Li yields an activation energy of 92.5 kJ/mol (22.1 kcal/mol) [3].

This paper reviews the corrosion data for ferritic HT-9 and modified Fe-9Cr-1Mo steel in flowing lithium and Pb-17Li environments at temperatures between 370 and 550 °C. Recent results for these alloys and several low-activation ferritic steels are presented. The effects of temperature and lithium purity on corrosion are discussed.

2. Experimental procedure

Corrosion tests were conducted in forced-circulation lithium and Pb-17Li loops. A detailed description of the loops and the test procedure have been presented earlier [1-4]. The chemical composition of the various ferritic steels is given in table 1. The temperature and time of

* Work supported by the US Department of Energy, Office of Fusion Energy, under Contract W-31-109-Eng-38.

Table 1
Chemical composition of ferritic steels

Alloy	Content (wt%)									
	Cr	Ni	Mo	Mn	Si	P	S	C	N	Other
HT-9	12.0	0.6	1.03	0.50	0.22	0.006	0.002	0.210	0.003	0.32 V, 0.5 W
Fe-9Cr-1Mo	8.8	–	0.92	0.40	0.36	–	–	0.098	0.011	0.2V, 0.06 Nb
Fe-9Cr-0.5V	9.13	–	–	0.02	0.09	0.005	0.003	0.010	0.003	0.52 V
Fe-9Cr-2.5Mn	8.82	–	–	2.44	0.10	0.005	0.004	0.101	0.002	0.27 V, 0.89 W
Fe-12Cr-6.5Mn	11.81	–	–	6.47	0.11	0.005	0.005	0.097	0.003	0.28 V, 0.89 W

Table 2
Lithium loop operating conditions for various corrosion tests

Test run	Loop temperatures (°C)				N content in Li (wppm)	Exposure time (h)	
	Test vessel	Spec. exp. vessel [a]	Supply vessel	Cold trap		Test vessel	Spec. exp. vessel
4	482	427	410	212	50–100	5521	6501
5	427	372	372	206	~100	5023	4955
6	538	482	410	208	~50	3655	3330
8	482	427	426	213	15–20	2158	2052

[a] Lithium flow was from test vessel to specimen exposure vessel.

exposure and the loop operating conditions for the tests in lithium are given in table 2. During Run 8, additional specimens of pure chromium, iron (Armco iron), nickel, and the alloy Fe–2.25Cr–1Mo were exposed to lithium. For all tests, lithium was circulated at ~1 *l*/min in the primary loop, and the concentrations of carbon and hydrogen in lithium were ~10 and 120 wppm, respectively. The nitrogen content is given in table 2.

Four corrosion tests of 2000- to 5500-h duration were conducted in Pb–17Li between 482 and 371°C. For each test, specimens were exposed at the maximum temperature position as well as at a downstream location. The Pb–17Li alloy was circulated at ~0.35 *l*/min. Several analyses of the eutectic alloy showed that the concentrations of hydrogen and nitrogen were 22 and < 10 wppm, respectively.

3. Results

3.1. Lithium environment

The weight losses of HT-9 and Fe–9Cr–1Mo steel exposed during various test runs at 482 and 427°C are shown in fig. 1. A steady-state dissolution behavior is achieved after an initial transient period. For both steels, the steady-state dissolution rates obtained from the different test runs are comparable. However, the weight losses of these steels after the transient period in runs 6 and 8 are lower than those for Runs 4 and 5. Furthermore, for Run 8, the weight losses of Fe–9Cr–1Mo steel are lower than those of the HT-9 alloy. The differences in the initial weight loss may be attributed to the chemical interactions between nitrogen and chromium. The nitrogen content in lithium during Runs 4 and 5 was ~100 wppm; during Run 8, it was 15 to 20 wppm.

Metallographic examination of HT-9 specimens exposed to lithium showed that the alloy develops a dimpled surface structure and the concentration of chromium in the surface decreases from ~12% to between 6 and 8%; the values after exposure at 538°C are lower than those at 371°C [2]. In general, the depletion of chromium is greater for specimens that show large weight loss, i.e., those exposed at high temperatures or to lithium with higher nitrogen content. Nitrogen can react with alloy elements and lithium to form ternary nitrides, such as Li_9CrN_5 and Li_3FeN_2. These ternary nitrides are soluble in alcohol or water, and therefore, are not observed on corrosion specimens after cleaning. The presence of ternary nitrides was investigated by chemical analysis of the alcohol used for cleaning the corrosion specimens [2]. The solutions contained significant amounts of chromium and iron. These results indicate that the chemical reactions between nitrogen and alloy elements increase the depletion of chromium and weight loss during the initial transient period. Such effects are more pronounced for alloys containing a higher concentration of chromium.

The influence of chemical interactions on the corrosion behavior of ferritic steels was investigated by exposing Fe–2.25Cr–1Mo ferritic steel and pure chromium, iron, and nickel to flowing lithium at 482 and 427°C (Run 8). At both temperatures, the nickel specimens (weighing ~0.6 g) dissolved completely in < 200 h. The weight losses for pure chromium, Armco iron, and Fe–2.25Cr–1Mo steel exposed to lithium at 42 and 427°C are shown in fig. 2; the negative values represent weight gain. At 482°C, the dissolution rate for Fe–2.25Cr–1Mo steel (0.14 mg/m^2 h) is 30 to 40% lower than that for HT-9 (~0.24 mg/m^2 h) or Fe–9Cr–1Mo steel (~0.19 mg/m^2 h). Similar variations in dissolution rates have also been observed at 538° [15]. Armco iron shows a weight gain after the initial 300-h exposure at 482°C and little or no weight loss for longer exposure times. The data for Armco iron yield a dissolution rate of 0.075 mg/m^2 h at 482°C. Pure chromium showed significant corrosion and was very brittle after exposure to lithium. At 482 and 427°C, the dissolution rates for pure chromium are about a factor of 8 greater than those for HT-9 or Fe–9Cr–1Mo steel.

The Fe–2.25Cr–1Mo and pure metal specimens were examined metallographically to characterize the composition and surface morphology after exposure to lithium. Micrographs of the surface of Armco iron, Fe–2.25Cr–1Mo, and chromium specimens exposed to lithium at 482°C, shown in fig. 3, reveal that the Armco iron and Fe–2.25Cr–1Mo specimens developed a di-

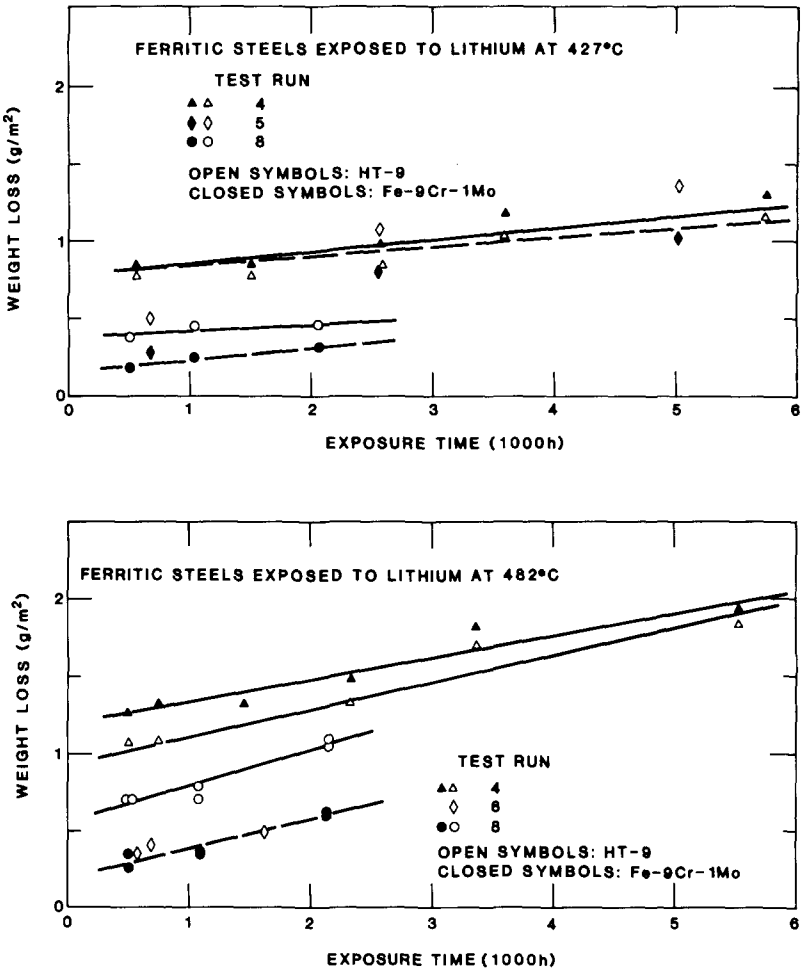

Fig. 1. Weight loss versus exposure time for HT-9 and Fe–9Cr–1Mo ferritic steels exposed to flowing lithium at 482 and 427 ° C.

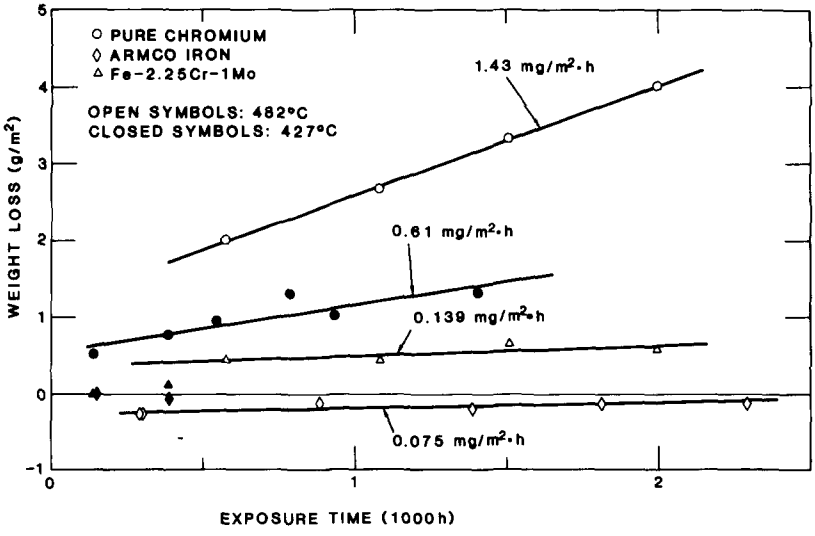

Fig. 2. Weight loss versus exposure time for pure chromium, Armco iron, and Fe–2.25Cr–1Mo steel exposed to flowing lithium at 482 and 427 ° C.

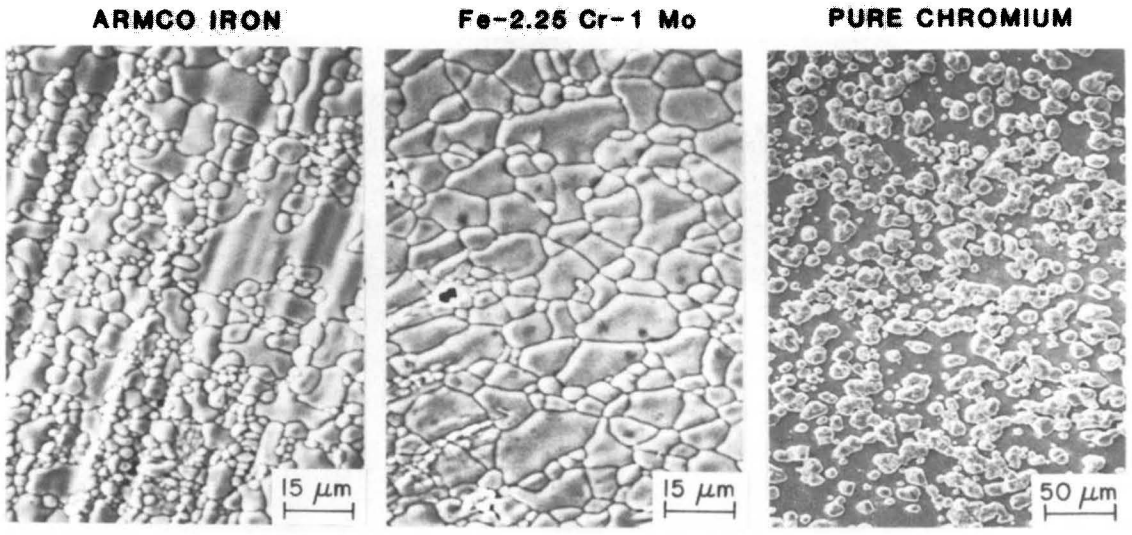

Fig. 3. Micrographs of the surface of corrosion specimens exposed to lithium at 482° C for ~ 2000 h.

mpled or etched appearance. Similar surface structure has been observed for Fe–2.25Cr–1Mo steel [15] and for HT-9 [2] exposed to lithium and seems to be characteristic of all Fe–Cr ferritic steels. Energy dispersive X-ray analyses showed slight increases in the chromium and nickel content of these specimens. A typical analysis of Armco iron exposed either at 482 or 427° C showed 0.7% Cr and 0.3% Ni at the surface. The Fe–2.25Cr–1Mo steel exposed to lithium for ~ 2000 h at 482° C contained 2.6% Cr compared to 2.2% Cr in the unexposed steel. An increase in chromium content from 2.2 to 5.6% has been observed for Fe–2.25Cr–1Mo steel exposed to lithium at 538° C for 948 h [15]. The weight change of these specimens, therefore, represents two competing processes, viz., weight gain from pickup of chromium and nickel from lithium and weight loss due to dissolution of iron from the alloy.

The surface of the chromium specimen is relatively smooth, but is covered with deposits. Such deposits were also observed on the specimen exposed at 427° C. A typical analysis of the chromium specimens showed ~ 1.0% Fe in the surface; the deposits also contained ~ 3.0% Ni. Surface deposits have been observed earlier on ferritic HT-9 and Fe–9Cr–1Mo steel or austenitic Type 316 stainless steel [2].

The weight losses for the low-activation ferritic steels

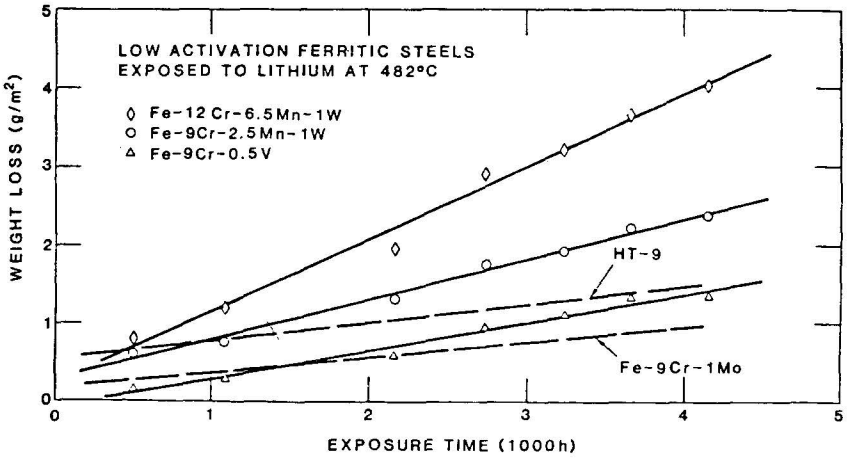

Fig. 4. Weight loss versus exposure time for low-activation ferritic steels exposed to flowing lithium at 482° C during Run 8.

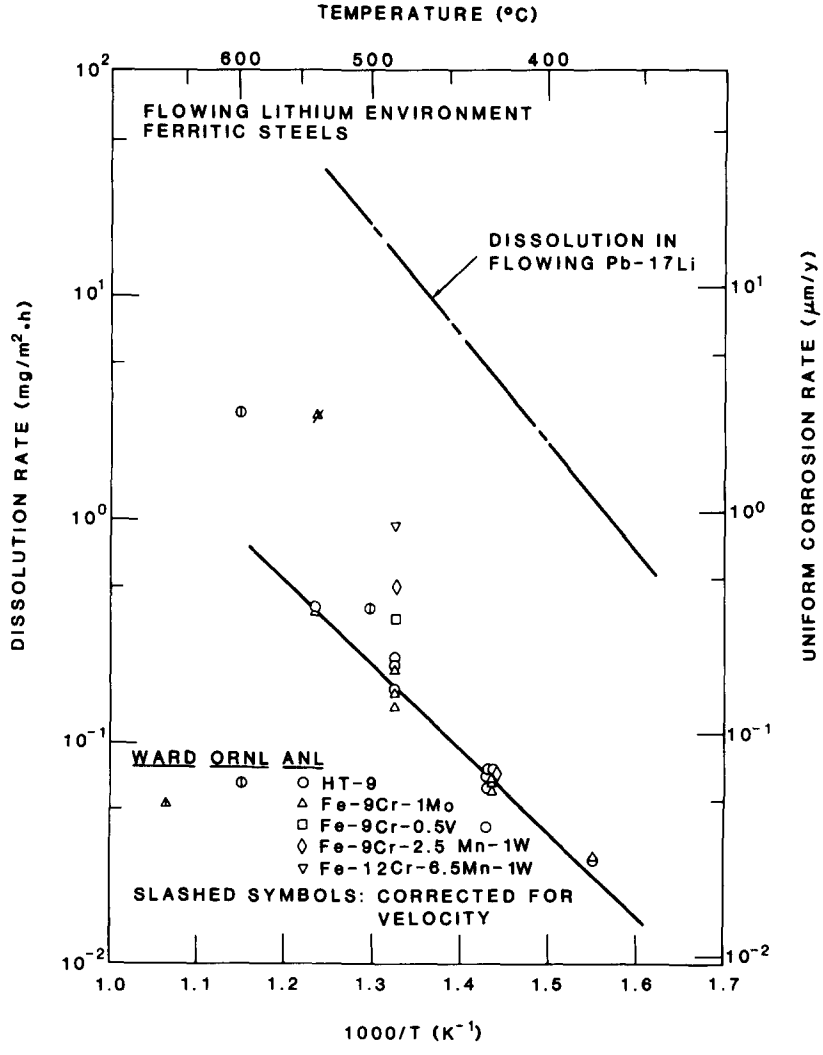

Fig. 5. Arrhenius plots of dissolution rate data for ferritic steels exposed to flowing lithium and Pb–17Li. ANL: Argonne National Laboratory; ORNL: Oak Ridge National Laboratory [18]; WARD: Westinghouse Advanced Reactor Division [15].

exposed to lithium at 482° C are shown in fig. 4. The Arrhenius plot of the steady-state dissolution rates for the various ferritic steels is shown in fig. 5. The corrosion data for HT-9 in a thermal convection loop at 500 and 600° C [17] and of Fe–9Cr–1Mo steel in a forced-circulation loop at 538° C [15] are also plotted in fig. 5. The results indicate that a maximum operating temperature of 550° C would yield a uniform corrosion rate of ~ 0.5 μm/yr. The dissolution rate of the Fe–9Cr–0.5V steel is comparable to that of HT–9 or Fe–9Cr–1Mo steel while the rates for the Mn-containing steels are a factor of 2 to 3 higher than for the other steels. The higher rates may be attributed to selective leaching of manganese from these steels. Depletion of manganese has been observed in various ferritic and austenitic steels exposed to flowing lithium [1,18].

3.2. Pb–17Li environment

The weight losses of HT-9 and Fe–9Cr–1Mo steel exposed at the maximum temperature positions at 482, 454, 427, and 371° C are shown in fig. 6. For both steels, the weight losses increase linearly with time and yield a constant dissolution rate. Specimens exposed at 482° C show significant weight loss after the initial 500-h exposure to Pb–17Li. The weight losses of low-activation ferritic steels exposed to Pb–17Li at 482 and 371° C are shown in fig. 7. The weight losses and dissolution rates of these steels are comparable to those of HT-9 or Fe–9Cr–1Mo steel.

The Arrhenius plot of steady-state dissolution rates for the various ferritic steels in Pb–17Li is shown in fig.

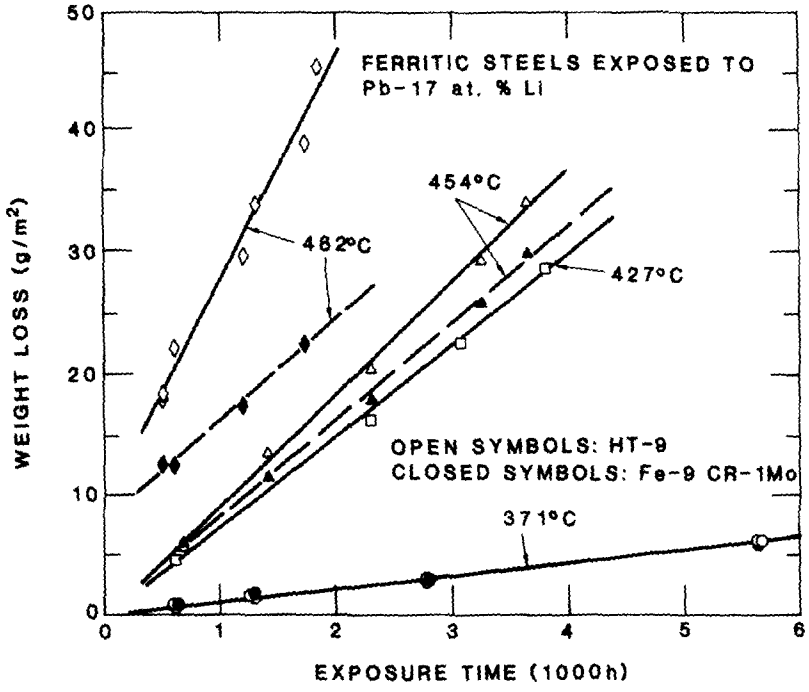

Fig. 6. Weight loss versus exposure time for HT-9 and Fe-9Cr-1Mo steel exposed to flowing Pb-17Li at the maximum loop temperature position.

5. The results yield an activation energy of 92.5 kJ/mol (22.1 kcal/mol). A maximum operating temperature of 550 ° C would result in a uniform corrosion rate of ~ 20 μm/yr, a rate approximately 40 times greater than in lithium.

4. Conclusions

The corrosion data indicate that dissolution of major elements as well as chemical reactions between nitrogen and alloy elements influence the corrosion behavior of

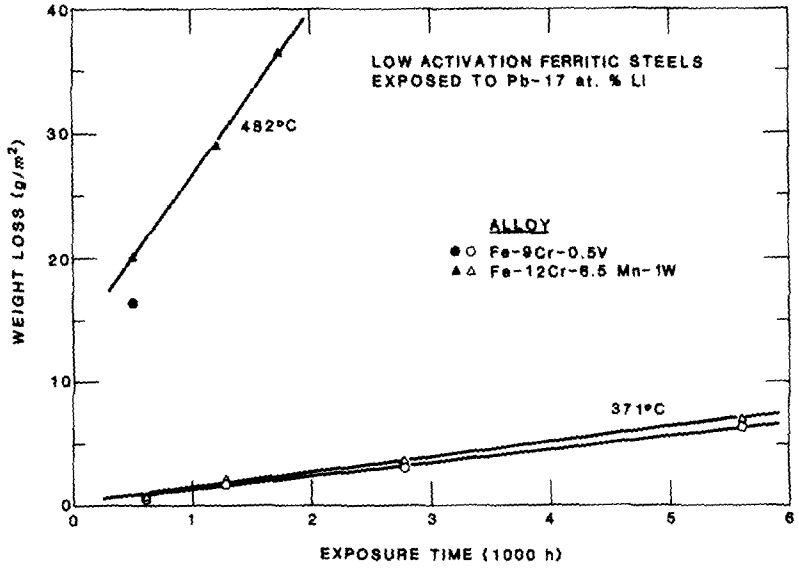

Fig. 7. Weight loss versus exposure time for low-activation ferritic steels exposed to flowing Pb-17Li at the maximum loop temperature position.

ferritic steels in flowing lithium. A steady-state dissolution rate is achieved after an initial transient period of ~ 500 h. The weight loss during the transient period is primarily controlled by chemical reactions and is dependent on the nitrogen content in lithium. After exposure to lithium, the ferritic steels undergo rapid changes in surface composition and develop a dimpled or etched appearance. The data indicate that the equilibrium surface composition for these steels in an austenitic stainless steel lithium system is ~ 6% Cr, ~ 1% Ni, and the balance Fe [2]. Consequently, ferritic steels with > 6% Cr lose chromium and steels with < 6% Cr pick up chromium during the initial transient period. An equilibrium surface composition of 8–10% Cr, 1–3% Ni, and 85–87% Fe has been reported for Fe–2.25Cr–1Mo and Fe–9Cr–1Mo steel exposed to lithium at 540 °C [19].

The steady-state dissolution rates for ferritic steels increase with an increase in temperature and are expressed by an Arrhenius plot with an activation energy of 68.2 kJ/mol. The dissolution rates of low-activation Fe–9Cr–0.5V steel are comparable to those of HT-9 and Fe–9Cr–1Mo steel whereas the rates of Mn-containing Fe–9Cr–2.5Mn or Fe–12Cr–6.5Mn steels are a factor of 2 to 3 higher. The dissolution rates of pure chromium are a factor of 8 greater than those of HT-9 alloy while the rates for Armco iron are slightly lower. After the initial transient period, Armco iron specimens show a weight gain due to the pickup of chromium and nickel from lithium.

The weight loss and steady-state dissolution rates of ferritic steels in flowing Pb–17Li are more than an order of magnitude greater than in lithium. The dissolution rates for the low-activation ferritic steels are comparable to those for HT-9 and Fe–9Cr–1Mo steel. The temperature dependence of dissolution rates of the various ferritic steels is expressed by an activation energy of 92.5 kJ/mol.

The authors acknowledge the experimental contributions provided by R.H. Lee. The low-activation ferritic steels were supplied by D.S. Gelles of Westinghouse Hanford Company. This work was supported by the US Department of Energy, Office of Fusion Energy, under Contract W-31-109-Eng-38.

References

[1] O.K. Chopra and D.L. Smith, J. Nucl. Mater. 133 & 134 (1986) 861.
[2] O.K. Chopra and D.L. Smith, J. Nucl. Mater. 141–143 (1986) 584.
[3] O.K. Chopra and D.L. Smith, J. Nucl. Mater. 141–143 (1986) 566.
[4] O.K. Chopra and D.L. Smith, J. Nucl. Mater. 122 & 123 (1984) 1219.
[5] O.K. Chopra and P.F. Tortorelli, J. Nucl. Mater 122 & 123 (1984) 1219.
[6] O.K. Chopra, D.L. Smith, P.F. Tortorelli, J.H. DeVan and D.K. Sze, Fusion Technol. 8 (1985) 1956.
[7] P.F. Tortorelli and J.H. DeVan, J. Nucl. Mater. 141–143 (1986) 592.
[8] P.F. Tortorelli and J.H. DeVan, in: Proc. Topical Conf. on Ferritic Alloys for Use in Nuclear Energy Technologies, Eds. J.W. Davis and D.J. Michel (AIME, 1984) p. 215.
[9] P.F. Tortorelli and J.H. DeVan, in: Proc. Third Int. Conf. on Liquid Metal Technology in Energy Production, 1984, Oxford, Vol. 3, p. 81.
[10] F. Casteels, J. Dekeyser, M. Soenen, H. Tas and J. Dresselaers, ibid. ref. [9] 73.
[11] H. Tas, J. Dekeyser, F. Casteels, J. Walnier and F. de Schutter, J. Nucl. Mater. 141–143 (1986) 571.
[12] M. Broc, P. Fauvet, T. Flament and J. Sannier, J. Nucl. Mater. 141–143 (1986) 61.
[13] H.V. Borgstedt, G. Frees and G. Drechsler, J. Nucl. Mater. 141–143 (1986) 561.
[14] H.V. Borgstedt, M. Grundmann and J. Konys, Fusion Technol. 8 (1985) 536.
[15] G.A. Whitlow, W.L. Wilson, W.E. Ray and M.G. Down, J. Nucl. Mater. 85 & 86 (1979) 283.
[16] V.I. Nikitin et al., USSR Contribution to INTOR Report, 1983, Appendix VI.
[17] P.F. Tortorelli and J.H. DeVan, J. Nucl. Mater. 141–143 (1986) 579.
[18] P.F. Tortorelli and J.H. DeVan, in: Alloy Development for Irradiation Performance: Semiannual Progress Report for Period Ending March 31, 1985, DOE/ER-0045/14, Oak Ridge National Laboratory, Oak Ridge, TN (July 1985) p. 197.
[19] C. Bagnall, J. Nucl. Mater. 103 & 104 (1981) 639.